



# Experimental validation of non-invasive and fluid density independent methods for the determination of local wave speed and arrival time of reflected wave

Ye Li, Ashraf W. Khir\*

Brunel Institute for Bioengineering, Brunel University, Kingston Lane, Uxbridge, Middlesex, UB8 3PH, UK

## ARTICLE INFO

### Article history:

Accepted 18 December 2010

### Keywords:

Non-invasive  
Diameter  
Velocity  
Pressure  
Validation  
InDU-loop

## ABSTRACT

The relationship between the vessel diameter ( $D$ ) and fluid velocity ( $U$ ) in arteries and flexible tubes has been recently characterized as linear in the absence of wave reflections. This relationship allowed for determining local wave speed ( $C_{DU}$ ) using the InDU-loop method. Using  $C_{DU}$ , it was possible to separate  $U$  and  $D$  waveforms into their forward and backward components. It was also possible to calculate wave intensity ( $dI_{DU}$ ), using  $D$  and  $U$ , from which the arrival time of reflected wave ( $Trw_{DU}$ ) could be determined. These techniques are fluid density independent and require only non-invasive measurements of  $D$  and  $U$ .

In this work we experimentally validate the relative accuracy of these new techniques *in vitro*, by comparing their results of  $C_{DU}$  and  $Trw_{DU}$  to those determined by the established techniques, PU-loop and wave intensity analysis,  $C$  and  $Trw$ , respectively. We generated a single semi-sinusoidal wave in long flexible tubes, and simultaneously measured pressure ( $P$ ),  $D$ , and  $U$  at the same site. Sequentially in time, we repeated this experiment at three sites along each of the flexible tubes, which were made of different materials and sizes, and three fluids of different densities.

$C_{DU}$  compared well with that  $C$  and likewise  $Trw_{DU}$  was very similar to  $Trw$ . Varying fluid density did not appreciably change the difference between the results of the two techniques.

We conclude that the new techniques for determining  $C_{DU}$  and  $Trw_{DU}$ , although independent of density, provide relatively accurate estimates of wave speed and arrival times of reflected waves *in vitro*. The new techniques require only non-invasive measurements of  $D$  and  $U$ , and further *in vivo* validation is required to establish its advantage in the clinical setting.

© 2011 Elsevier Ltd. All rights reserved.

## 1. Introduction

Wave speed ( $C$ ) is the speed by which disturbance travels along the medium, and it is well accepted as one of the key parameters describing wave propagation in arteries (McDonald, 2007).  $C$  depends chiefly upon the local properties of the arterial wall (Bergel, 1961) and widely used clinically to determine arterial stiffness (Asmar et al., 1995). Further,  $C$  increases with aging (Mohiaddin et al., 1993) and has been associated with cardiovascular diseases such as atherosclerosis and arteriosclerosis (Blacher et al., 1999).

Several methods have been proposed for the determination of local wave speed. Westerhof et al. (1972) suggested that the ratio of magnitudes of pressure ( $P$ ) to flow velocity ( $U$ ), and the characteristic impedance, can be used to determine  $C$ . They

argued that for the higher harmonics the effect of reflected sinusoidal wave-trains will be negligible, and the characteristic impedance indicates  $C$ . Khir et al. (2001a) used the water hammer equation and introduced the PU-loop method for determining  $C$ . They argued that in the absence of reflections the relationship between pressure and velocity should be linear and the slope of the initial linear portion of the loop is related to  $C$ . To deal with reflections, Davies et al. (2006) introduced the sum of the squares technique for determining  $C$  in shorter arterial segments. The application of the above methods requires simultaneous measurements of  $P$  and  $U$  at the same site. This requirement may not be practical in the clinical setting, due to the invasive nature of collecting reliable pressure measurements.

The arrival time of reflected wave ( $Trw$ ) to the ascending aorta is another parameter that is of clinical and physiological importance. For example,  $Trw$  has been used to diagnose ventricular hypertrophy and cardiac failure (Koh et al., 1998). Earlier arrival of reflected compression waves suggests higher wave speed and causes an increase in  $P$ , which is thought to increase left ventricle

\* Corresponding author. Tel.: +44 0 1895265857; fax: +44 0 1895274608.  
E-mail address: [ashraf.khir@brunel.ac.uk](mailto:ashraf.khir@brunel.ac.uk) (A.W. Khir).

(LV) afterload (Khir et al., 2001b). This increase may augment LV oxygen demands in order to maintain cardiac output (Kelly et al., 1992).

Several methods have been proposed for the determination of Trw. Murgo et al. (1980) suggested that time of the inflection point on the upstroke of the pressure waveform represented Trw. Parker and Jones (1990) introduced wave intensity analysis (WIA), which is a time domain technique, and allows for the separation of the forward and backward  $P, U$  waveforms and wave intensities ( $dI_{PU}$ ). WIA thus can be used for the determination of Trw, and has been applied to different sites in the cardiovascular system; aorta (Koh et al., 1998), coronary arteries (Sun et al., 2000), and left and right ventricular (Wang et al., 2005). WIA has been shown to accurately estimate Trw *in vitro* (Khir and Parker, 2002) and *in vivo* (Khir and Parker, 2005). However, both the inflection point and WIA methods require a reliable measurement of local pressure.

Feng and Khir (2010) have developed novel techniques using the non-invasive measurements of  $U$  and the vessel diameter ( $D$ ) for the determination of  $C$  and Trw. The authors demonstrated that the relationship between  $\ln D$  and  $U$  is linear in the absence of reflections and the slope of the  $\ln DU$ -loop is linear in the early part of the cycle when only forward waves are present. It is worth noting that this method is independent of the fluid density. Using  $D, U$ , and  $C$ , the authors also introduced a technique for the separation of the forward and backward  $D, U$  waveforms and non-invasive wave intensities ( $dI_{DU}$ ), which can also be used to estimate Trw.

Given the variety of different methods and the lack of comparisons between them, the aim of this work is therefore to experimentally test the relative accuracy of the  $\ln DU$ -loop

method for measuring  $C$ , and the  $dI_{DU}$  method for estimating Trw in flexible tubes as compared with the  $PU$ -loop and  $dI_{PU}$  methods.

2. Methods

In this work we refer to  $C$  determined using the  $\ln DU$ -loop method as ( $C_{DU}$ ) and that determined using the  $PU$ -loop method as ( $C_{PU}$ ). Also, we refer to Trw determined using  $dI_{DU}$  as ( $Trw_{DU}$ ) and that determined using  $dI_{PU}$  as ( $Trw_{PU}$ ). Further, subscripts of (+) and (-) indicate the forward and backward direction, respectively. The derivation of the methods used to calculate  $C_{DU}, C_{PU}, Trw_{DU}$ , and  $Trw_{PU}$  have been described in previous works (Parker and Jones, 1990; Khir et al., 2001a; Feng and Khir, 2010) but the equations used by each method are compared in Table 1.

2.1. Experimental setup

The general experimental setup of this study is shown in Fig. 1 and a description of the individual elements is as follows.

2.1.1. Tubes

We used flexible tubes of different materials and sizes, whose dimensions are given in Table 2. The mechanical properties of each tube are uniform along its 1 m length. The tubes were fully immersed in a water tank and all experiments were carried out in the horizontal position.

2.1.2. Pump

The inlet of each tube was connected to a piston pump, which produced an approximately semi-sinusoidal single pulse wave with the piston moving forward from the bottom to the top dead center. The cylinder of the pump is 5 cm in diameter and the stroke of the piston is 2 cm; giving a displaced volume of approximately 40 ml.

Table 1 The expressions of  $P, U$ , and  $D, U$  based techniques for the determination of wave speed ( $C$ ), the separation of waves and wave intensity.

	$P, U$ based equations	$D, U$ based equations
Wave speed	$c = \pm \frac{1}{\rho} \frac{dP_{\pm}}{dU_{\pm}}$	$c = \pm \frac{1}{2} \frac{dU_{\pm}}{d \ln D_{\pm}}$
Forward and backward changes in $P$ and $D$	$dP_{\pm} = \pm \frac{1}{2} (dP \pm \rho c dU)$	$dD_{\pm} = \pm \frac{1}{2} (d \ln D \pm \frac{1}{2c} dU)$
Forward and backward $P$ and $D$ waveforms	$P_{\pm} = \sum_{t=0}^t dP_{\pm} + P_0$	$D_{\pm} = \sum_{t=0}^t dD_{\pm} + D_0$
Forward and backward changes in $U$	$dU_{\pm} = \pm \frac{1}{2} (\frac{dP}{\rho c} \pm dU)$	$dU_{\pm} = \pm \frac{1}{2} (dU \pm 2c d \ln D)$
Forward and backward $U$ waveforms	$U_{\pm} = \sum_{t=0}^t dU_{\pm}$	$U_{\pm} = \sum_{t=0}^t dU_{\pm}$
Forward and backward wave intensity	$dI_{PU_{\pm}} = \pm \frac{1}{4\rho c} (dP \pm \rho c dU)^2$	$dI_{DU_{\pm}} = \pm \frac{c}{2} (d \ln D \pm \frac{1}{2c} dU)^2$

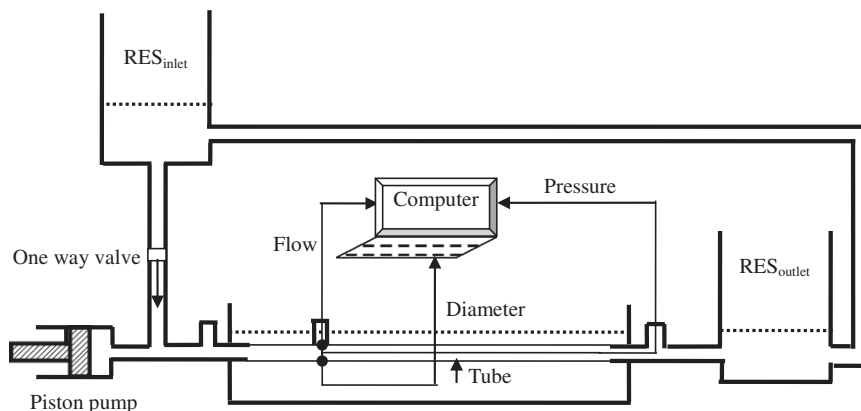


Fig. 1. A schematic diagram of the experimental setup. RES<sub>inlet</sub> and RES<sub>outlet</sub> are the inlet and outlet reservoirs, which provided the initial pressure to the system, and kept the tube free of air. Pressure and flow were measured using transducer tipped catheters, and ultrasonic flow meter and probes, respectively. Diameter was measured using a pair of ultrasound crystals. All elements of the experiment are placed on the horizontal plane so that the heights of the inlet and outlet reservoirs were equal.

2.1.3. Reservoirs

The inlet and outlet reservoirs were interconnected, and the height of the fluid in the reservoirs was adjusted to 10 cm above the longitudinal axis of the tube; producing an initial hydrostatic pressure of 1 KPa. We note that although the transmural pressure for the different-sized tubes will vary, this variation was ignored as it was not significant and its effect was expected to be minimal. The experimental tubes were connected to the reservoirs using rigid polyurethane tubing. A one-way valve was placed between the outlet of reservoir and the inlet of each tube, as shown in Fig. 1, to prevent any portion of the displaced volume from flowing directly into the reservoir.

2.1.4. Fluids

Experiments were carried out for three fluids with different densities, water (1000 kg/m<sup>3</sup>), 50% and 75% glycerin–water solution (1126.3 and 1194.9 kg/m<sup>3</sup>).

**Table 2**

Materials and dimensions of the tubes used in the experimental validation. Also shown are the average wave speeds measured in each tube with water ( $\rho = 1000 \text{ kg/m}^3$ ).

Material	Internal diameter (D) (mm)	Wall thickness (h) (mm)	$C_{DU}$ (m/s)	$C_{PU}$ (m/s)
Silicone	8	1	22.27	21.95
		2	26.67	28.67
		3	33.46	31.99
	10	1	19.96	20.22
		2	25.30	24.28
		3	29.86	30.17
16	2.4	22.43	21.85	
	3	25.12	23.05	
Rubber	16.7	1.5	23.89	24.17
	20.6	1.5	20.73	20.85
Latex	8.5	0.1	5.16	5.36
	24.2	0.27	3.11	2.94
	32.3	0.27	2.60	2.61

2.1.5. Measurements

Simultaneous waveforms of pressure (P), outer diameter (D<sub>o</sub>), and flow (Q), from which D and U were determined, were measured sequentially in time at three different sites, 25, 50, and 75 cm away from the inlet of each tube. P and Q were measured using 8F tipped catheter pressure transducer (Millar Instruments, Texas, USA) and ultrasonic flow probe (Transonic System, Inc, NY, USA), respectively. D<sub>o</sub> was measured using paired ultrasonic crystals (Sonometrics Corporation, Ontario, Canada), and wall thickness was measured using a digital caliper. All data were sampled at 500 Hz using Sonolab (Sonometrics Corporation) and analyzed using Matlab (The Mathworks, MA, USA).

2.2. Analysis

Because we used tubes with a range of diameter (D) and wall thickness (h), a normalization parameter, h/D was used, to compare C<sub>DU</sub> in different tubes. Trw was determined as the sampling point indicating time of the onset of the backward pressure (P<sub>-</sub>), velocity (U<sub>-</sub>), diameter (D<sub>-</sub>), and backward intensities  $dl_{PU-}$  or  $dl_{DU-}$ . Regression and paired t-test analyses were performed to identify the correlation between C<sub>PU</sub> and C<sub>DU</sub>, and between Trw<sub>DU</sub> and Trw<sub>PU</sub> to indicate the relative accuracy of the new technique compared to the established techniques. Data are presented as mean ± SD and values of p < 0.05 were considered significant. We also used the Bland–Altman technique (Bland and Altman, 1986) to establish the agreement between P, U, and D, U based techniques, and the acceptable range for the mean difference was taken as ± 2 SD.

3. Results

3.1. Wave speed

Fig. 2 shows P, U, and D waveforms and the corresponding PU-loop and InDU-loop measured at 50 cm away from the inlet of a rubber tube. The initial portion of the InDU-loop is clearly linear and the slope corresponds to C<sub>DU</sub> of 24.13 m/s. C<sub>PU</sub> measured at the same site is 24.58 m/s, and the difference between the results of both methods is 0.45 m/s (~2%), which is very small considering the level of experimental noise.

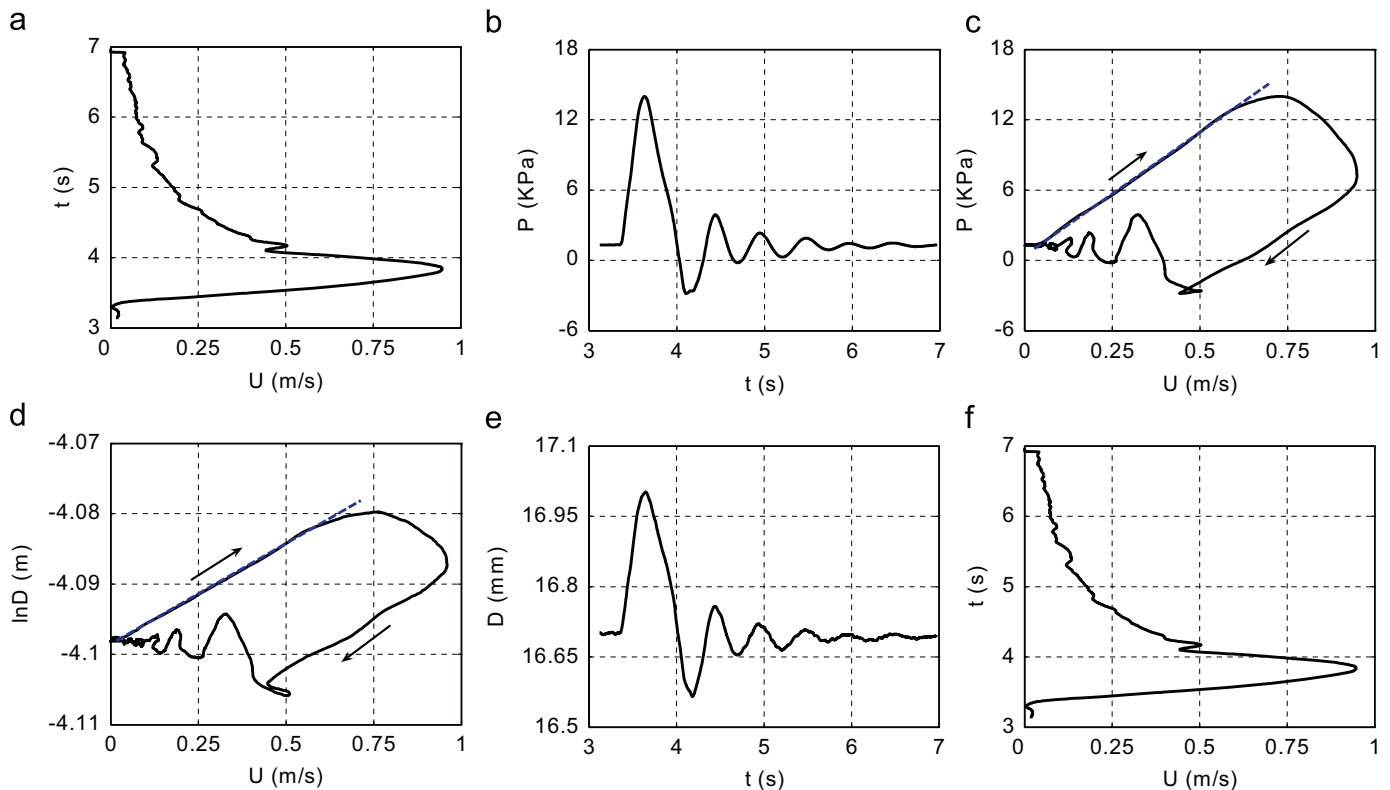


**Fig. 2.** The pressure (b), diameter (e) and velocity (a,f) waveforms measured at 50 cm away from the inlet of 1 m length rubber tube. The tube is 16.7 mm in diameter (unloaded) and 1.5 mm in wall thickness. The PU-loop is shown in (c) and InDU-loop is shown in (d) indicating wave speed of 24.58 and 24.13 m/s, respectively. The dashed line indicates the initial linear portion of each loop, and the arrows show the direction of the loop.

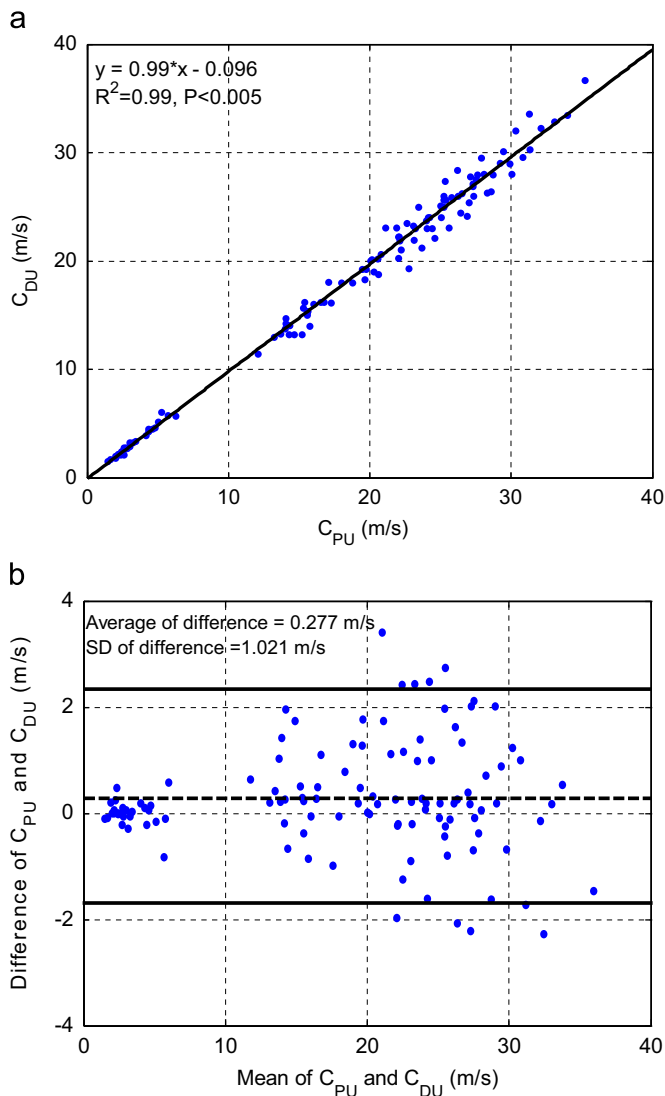


**Fig. 3.** (a) Correlation of wave speed determined by InDU-loop and PU-loop. The correlation coefficient  $R^2=0.99$ ,  $p < 0.005$  and (b) the agreement between wave speed determined by the InDU-loop and PU-loop is assessed by the Bland–Altman method. The middle horizontal line (dashed) indicates the mean of difference of wave speed determined by the two methods. The upper and lower horizontal lines (solid) indicate twice the standard deviation (2 SD). Note that most of the data points fell within  $\pm 2$  SD range, and the zero line fell within the acceptable confidence limits of the average, indicating no statistically significant difference between  $C_{DU}$  and  $C_{PU}$ .

Values of  $C_{DU}$  and  $C_{PU}$  in all of the tubes, locations, and fluid densities highly correlated ( $R^2=0.99$ ,  $p < 0.005$ ); Fig. 3a. The results of the InDU-loop and PU-loop methods are in agreement and the difference between  $C_{DU}$  and  $C_{PU}$  is within the acceptable range of mean  $\pm 2$  SD ( $0.28 \pm 2.04$  m/s); Fig. 3b.

Mean values of  $C_{DU}$  and  $C_{PU}$  measured in all of the tubes using water ( $\rho=1000$  kg/m<sup>3</sup>) are shown in Table 2. As expected,  $C$  decreased in tubes with larger diameter and smaller wall thickness. Mean values of  $C_{DU}$  measured in all of the tubes using water, 50% and 75% glycerin–water solutions are shown in Fig. 4.  $C_{DU}$  is slower with increased fluid density independent from  $h/D$ .

### 3.2. Wave separation

The measured, forward and backward pressure waveforms ( $P$ ,  $P_+$ ,  $P_-$ ) are very similar in shape to the corresponding ( $D$ ,  $D_+$ ,  $D_-$ ); Fig. 5a,b. Similarly, the shape of the forward and backward

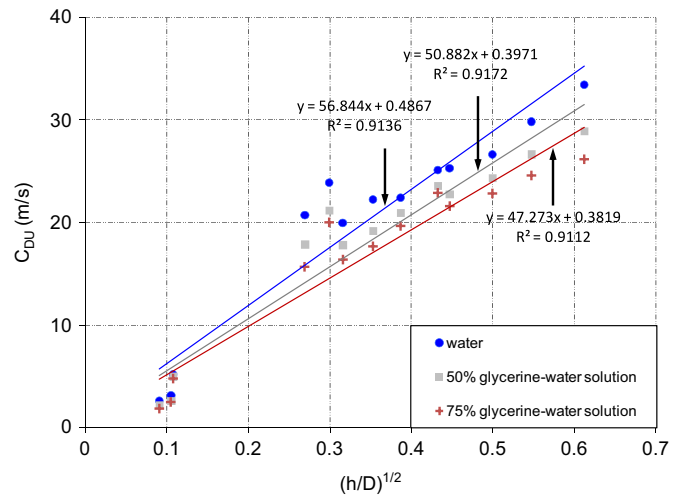


**Fig. 4.** Average wave speed for each tube determined using the InDU-loop method ( $C_{DU}$ ) is plotted against the square root of the normalization ratio of wall thickness to diameter ( $h/D$ ). Although the method is independent of fluid density,  $C_{DU}$  changes as expected; increases with increased  $h/D$  and also with decreased fluid density for each tube.

velocity ( $U_+$ ,  $U_-$ ) as determined by both techniques is almost identical; Fig. 5c,d. Also the shape of  $dl_{PU}$  and  $dl_{DU}$  in the forward and backward directions is very similar; Fig. 5e,f. All backward waveforms in Fig. 5, ( $P_-$ ,  $D_-$ ,  $U_-$ ,  $dl_{PU-}$ , and  $dl_{DU-}$ ) indicate the same Trw of 0.2 s.

### 3.3. Arrival time of reflected waves

Values of  $Trw_{PU}$  and  $Trw_{DU}$  highly correlated ( $R^2=0.98$ ,  $p < 0.02$ ) and the results of both methods are in agreement; Fig. 6. The average of difference between  $Trw_{PU}$  and  $Trw_{DU}$  is  $-0.0006$  s  $\pm$  0.007, and the agreement limit (mean  $\pm 2$  SD) of  $-0.015$ – $0.013$  s is small and provides confidence that the two methods are in agreement without bias.

## 4. Discussion

In this paper, we experimentally test a new method for the determination of wave speed and the separation of forward and backward waves using measurements of diameter and velocity. Wave speeds determined by the InDU-loop method are compared to those determined by the PU-loop method. The results of the two methods agree well and the small differences between the results of the two methods could not be attributed to any specific reason.

Flexible tube waves involve exchange between the kinetic energy of the fluid within the tube and the potential energy of the distending tube walls. Therefore, changes in  $P$ ,  $U$ , and  $D$  in flexible tubes are inextricably linked and a change in any of these parameters will induce a change in the other two. The distension of the tube wall is associated with a change in pressure and therefore the waves can be described either as pressure–velocity waves or as diameter–velocity waves. In the work of previous investigators, waves were described in terms of  $P$  and  $U$ , and in this work we present the waves in terms of  $D$  and  $U$  for the useful non-invasive benefits. Further, the term “intensity” does not have natural fundamental units, and evidently there are two methods using  $P$  and  $U$  giving wave intensity in different units; ( $W/m^2$ ) as described by Parker and Jones (1990) and ( $W/m^2 s^2$ ) as described by Ramsey and Sugawara (1997). Therefore, quite apart from the shape similarity between the curves produced by the previously

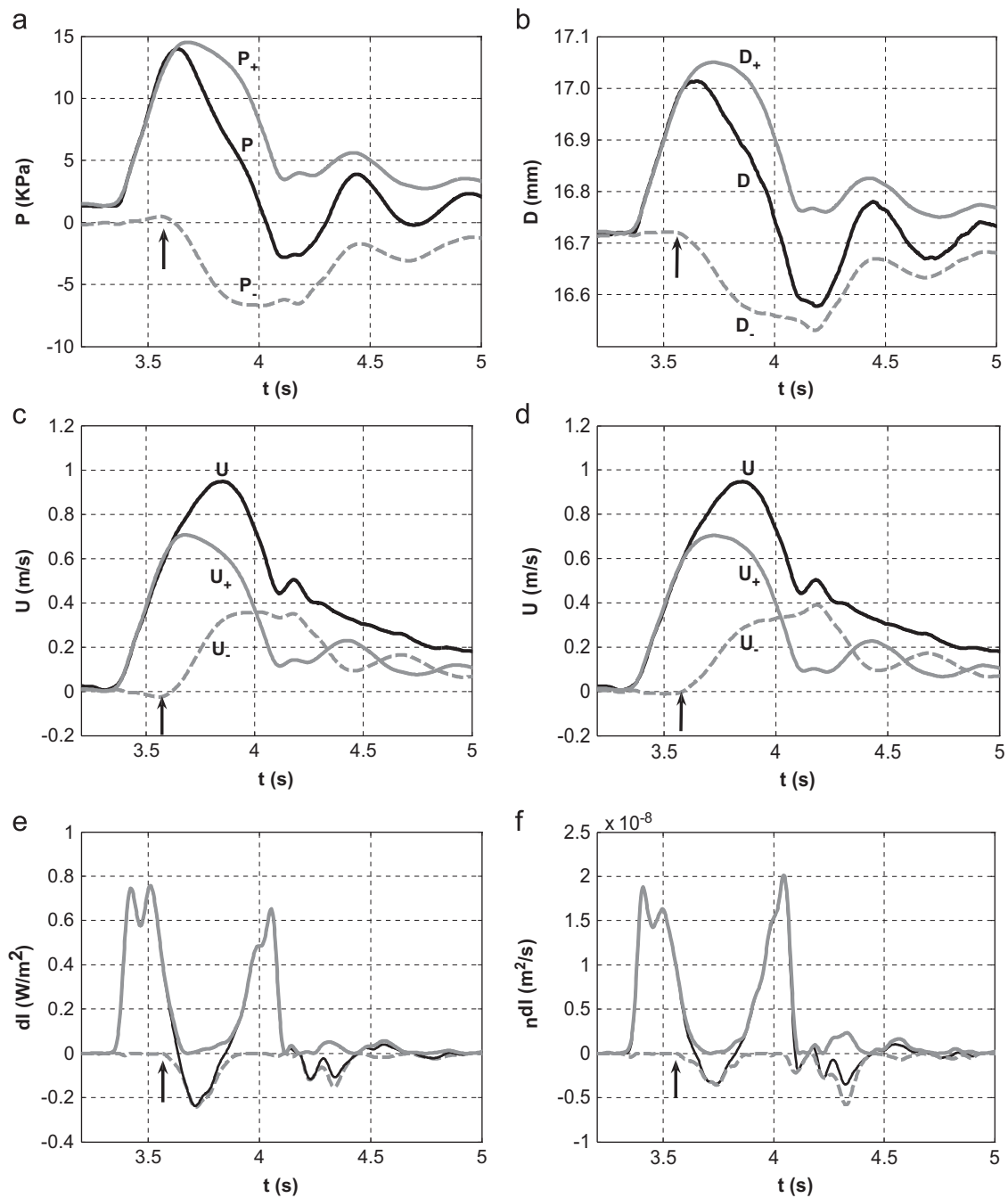


**Fig. 5.** The measured, calculated forward (+) and backward (–) pressure ( $P$ ), velocity ( $U$ ), and wave intensity ( $dl_{PU}$ ) using the  $PU$  equations are plotted against time (left). The measured, calculated forward and backward diameter ( $D$ ), velocity ( $U$ ), and non-invasive wave intensity ( ${}_n dl_{DU}$ ) using the  $DU$  equations (right). The dark lines show the measured parameters, gray lines show the forward waveforms and dashed lines shows the backward waveforms. The arrival time of the reflected waves ( $Trw$ ) detected by the onset of  $dl$  and  ${}_n dl$  correspond to the onset of the backward pressure, diameter, and velocity waves as indicated by the vertical arrows.

and currently introduced WIA, describing the waves using  $D$  and  $U$  as intensity with units of  $m^2/s$  is a natural approach that does not contradict any of the other methods.

In the current work, we define the elemental waves by the changes in diameter ( $dD$ ) and velocity ( $dU$ ). We also define the direction of the waves as positive in the direction of the mean flow. In line with the well establish notations in gas dynamics, waves for which  $dP > 0$  and  $dD > 0$  (wall extension) are termed “compression waves” and waves for which  $dP < 0$  and  $dD < 0$  (wall contraction) are termed “decompression” waves. The effect of these waves on velocity depends upon their direction; both forward compression and backward decompression waves cause

acceleration  $dU > 0$  while both forward decompression and backward compression waves cause deceleration,  $dU < 0$ . The inter-relations between fluid and diameter waves are defined in Table 3.

Determination of  $C$  and  $Trw$  non-invasively has recently attracted the interest of several researchers. Harada et al. (2002) presented an on-line one-point measurement method to determine  $C$  non-invasively; the principle of the method is to derive pulse wave velocity from the stiffness parameter of the artery. They measured the diameter-change of the carotid artery, calibrated the maximal and minimal values of the diameter waveform using systolic and diastolic blood pressure measured with a cuff-type manometer at the upper arm, and then substituted the

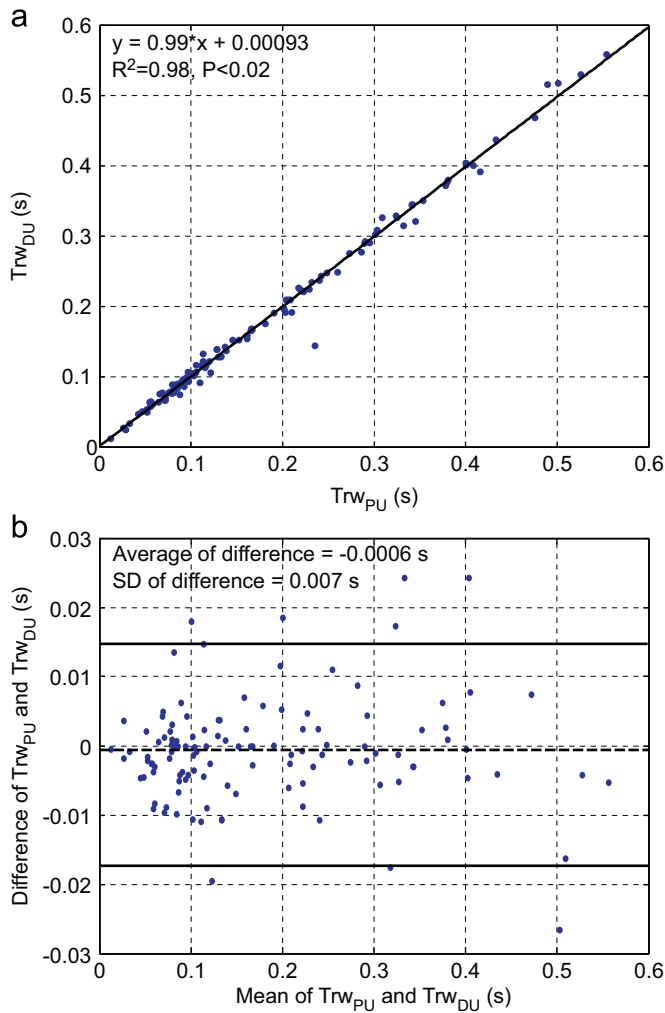


**Fig. 6.** In (a)  $Trw_{DU}$  and  $Trw_{PU}$  correlate well ( $R^2=0.98$ ,  $p < 0.02$ ) and the trend line appears to fall on the identity line (not shown). In (b) the Bland–Altman plot shows the agreement between the two results. The middle horizontal (dashed) line indicates the mean difference between the two methods. The upper and lower horizontal lines (solid) indicate twice the standard deviation (2 SD) of the mean difference. Note that most of the data points fell within  $\pm 2$  SD range, and the zero line fell within the acceptable confidence limits of the average, indicating no statistical significant difference between  $Trw_{DU}$  and  $Trw_{PU}$ .

**Table 3**

The inter-relations between fluid and diameter waves. Compression waves are associated with an increase in pressure and diameter, cause acceleration if running in the forward and deceleration if running in the backward direction. Decompression waves are associated with a decrease in pressure and diameter, cause acceleration if running the backward- and deceleration if running in the forward direction.

Waves nature	Wave effect	
	Forward (+)	Backward (-)
Compression	$dP > 0$	$dP > 0$
	$dD > 0$	$dD > 0$
	$dU > 0$	$dU < 0$
Decompression	$dP < 0$	$dP < 0$
	$dD < 0$	$dD < 0$
	$dU < 0$	$dU > 0$

calibrated diameter waveform for the pressure waveform. Hence, the stiffness parameter can be obtained simultaneously. Also, Meinders et al. (2001) introduced a multiple M-line system to

assess local pulse wave velocity, which was determined as the ratio of the temporal and spatial gradient of adjacent distension velocity waveforms that were determined simultaneously along a short arterial segment using a single 2D-vessel wall tracking. The advantage of this approach is that the segment length is set by the characteristics of the ultrasound probe and does not vary over measurements. Further, Rabben et al. (2004) presented a method for estimating  $C$  from ultrasound measurements; the flow-area loop method, in which  $C$  is estimated as the ratio between the change in flow to the change in cross-sectional area during the reflection-free period of the cardiac cycle. This method is similar to the method examined in this paper (InDU-loop) as  $C$  is determined from the linear portion of the loop during the reflection-free period of the cardiac cycle. It is worth noting that although the range of  $\ln D$  is small, Fig. 2, the number of data points making the initial linear part of the InDU-loop ( $n=116$ ) are approximately the same as those making the initial linear part of the PU-loop ( $n=115$ ). This evidently did not affect the relative accuracy between the InDU-loop and the PU-loop methods for calculating  $C$ , as shown in Fig. 3.

Whilst using the PU-loop method and WIA for the determination of  $C$  and  $Trw$  requires an estimation of  $\rho$ , the new techniques for their determination are independent of  $\rho$  as shown in Table 1. In this work we repeated the experiments using three fluids with different densities to examine the relative accuracy of the InDU-loop method to determine  $C$ . The densities we used were chosen in order to simulate a range of blood density; in human blood density is approximately  $1060 \text{ kg/m}^3$  (Cutnell and Johnson, 1998), the density of blood plasma is approximately  $1025 \text{ kg/m}^3$  and the density of blood cells circulating in the blood is approximately  $1125 \text{ kg/m}^3$  (Benson and Katherine, 1999). Fluid densities of 75% ( $\rho=1194.9 \text{ kg/m}^3$ ) and 50% ( $\rho=1126.3 \text{ kg/m}^3$ ) of glycerin–water solution are approximately 19.5% and 12.6%, respectively greater than that of water ( $\rho=1000 \text{ kg/m}^3$ ). Therefore using the Barnwell Hill equation, where  $D_s$  is distensibility, it is expected that  $C$  in 75% and 50% glycerin–water solutions to be 8.5% and 6%, respectively, smaller than that in water. The experimental results are in agreement with this prediction; for example, in the 16 mm diameter, 3 mm wall thickness silicone tube, we measured  $C_{DU}$  using 75 and 50% glycerin–water solution of 22.89 and 23.56 m/s, which shows 8.9% and 6.2% reduction of wave speed as compared with that measured in water, 25.12 m/s. The small differences between the theoretical and experimental results are acceptable within the experimental noise.

The results shown in Figs. 3a, and 6a also indicate a good agreement between the  $P$ ,  $U$ , and  $D$ ,  $U$  based techniques for the determination of  $C$  and  $Trw$ . In assessing the relationship between both methods, the results for both  $C_{PU}$  and  $C_{DU}$ , and  $Trw_{PU}$  and  $Trw_{DU}$  are highly correlated with the trend lines falling almost on top of the identity line. Figs. 3b and 6b show clearly that most of the data points fell between the acceptable range of difference and were well distributed, with no bias, around the mean difference, which is close to the zero line; all indicating no significant difference between the results of the two techniques. The results of  $C_{DU}$  and  $Trw_{DU}$  are not only in agreement with those of  $C_{PU}$ , and  $Trw_{PU}$ , but also in agreement with earlier work. For example, Khir and Parker (2002) reported  $C_{PU}$ , in a 1" (25.4 mm) diameter and 0.25 mm wall thickness latex tube using the PU-loop method to be  $3.4 \pm 0.8 \text{ m/s}$ . In this work,  $C_{DU}$  measured in a 24.2 mm diameter, 0.27 mm wall thickness latex is  $3.11 \pm 0.5 \text{ m/s}$ . Furthermore, Wang et al. (2009), using the foot-to-foot method reported  $C$  in a  $D_o=19.0 \text{ mm}$  and  $h=3.18 \text{ mm}$  elastic tube is  $25.3 \pm 0.2 \text{ m/s}$ . In our experiment,  $C_{DU}=29.86 \text{ m/s}$  in a  $D_o=16.0 \text{ mm}$  and  $h=3.0 \text{ mm}$  silicone tube. Given the differences in  $D$  and  $h$  the, results of this work are considered comparable to those obtained by other investigators using different methods.

Table 2 shows that tubes of different material and different  $h/D$  ratios yielded very similar wave speed. For example  $C_{DU}$  measured in a 16.7 mm diameter rubber tube with  $h/D$  of 0.09 was very similar to that measured in a 16 mm diameter silicone tube with  $h/D$  of 0.15. This can be understood through the Moens–Korteweg equation:  $C^2 = (Eh/\rho D)$ , where  $E$  is Young's Modulus. Bessems et al. (2008) used the same concept where they changed the wall thickness along the length of a tapered flexible tube to obtain constant  $C$ , which is similar to that measured in a straight tube of the same material. The results presented in the present paper further confirm that the  $\ln DU$ -loop is insensitive to changes of tubes dimensions and fluid density.

WIA provides a novel perspective on wave propagation along the ventricular–arterial system. The separation of instantaneous  $P$  and  $U$ , or  $D$  and  $U$  into their forward and backward traveling components allows for the quantitative assessment of the contribution of the ejecting left ventricle and of reflected waves from peripheral arteries. Accurate prediction of  $\text{Trw}$  is of clinical significance as it gives an indication to the mechanical properties of the arterial bed. However, almost all methods used for the determination of  $\text{Trw}$  require the invasive measurement of  $P$ , which is not practical in the clinical setting and may not be accurate enough if obtained non-invasively. The new techniques using  $D$ ,  $U$  based measurements offers a way for the determination of  $C$  and  $\text{Trw}$  non-invasively.

#### 4.1. Limitations

The strong agreement between the results of the  $PU$ -loop and the  $\ln DU$ -loop methods for determining  $C$  and between  $dI_{PU}$  and  $dI_{DU}$  for determining  $\text{Trw}$  are probably due to the properties of the tubes tested in this work. The relationship between  $P$  and  $D$  in the tubes we tested is linear indicating the walls are elastic over the range of pressures involved. However, the arterial wall is known to be viscoelastic and therefore further *in vivo* validation is required to establish the relative accuracy of the new techniques for clinical measurements.

## 5. Conclusions

The  $\ln DU$ -loop method for determining wave speed ( $C$ ) provided comparable and consistent results to those provided by the  $PU$ -loop method, over a range of different diameters and wall thicknesses of flexible tubes. Also, the results of non-invasive wave intensities ( $dI_{DU}$ ) for the determination of arrival time of reflected wave ( $\text{Trw}$ ) are very close to those calculated by wave intensities ( $dI_{PU}$ ). The  $\ln DU$ -loop and the  $dI_{DU}$  methods used for the determination of  $C$  and  $\text{Trw}$ , respectively, appear insensitive to the absence of a density term in their respective equations. The new techniques are able to separate the forward and backward diameter ( $D$ ) and velocity ( $U$ ) waveforms that appear typical to that traditionally used by impedance techniques or wave intensity analysis (WIA) for the separation of pressure ( $P$ ) and  $U$  waveforms. The new techniques based on  $D$  and  $U$  provide an integrated non-invasive system for studying waves traversing flexible tubes, requiring non-invasive measurements, and hence may have an advantage in the clinical setting, for which further *in vivo* validation is required.

## Conflict of interest statement

None declared.

## References

- Asmar, R., Benetos, A., Topouchian, J., Laurent, P., Pannier, B., Brisac, A.M., Target, R., Levy, B.I., 1995. Assessment of arterial distensibility by automatic pulse wave velocity measurement. *Hypertension* 26, 485–490.
- Benson, Katherine, 1999. MCAT Review. Emory University.
- Bergel, D.H., 1961. The static elastic properties of the arterial wall. *Journal of Physiology* 156, 445–457.
- Bessems, D., Giannopapa, C.G., Rutten, M.C.M., van de Vosse, F.N., 2008. Experimental validation of a time-domain-based wave propagation model of blood flow in viscoelastic vessels. *Journal of Biomechanics* 41, 284–291.
- Blacher, J., Asmar, R., Djane, S., London, G.M., Safar, M.E., 1999. Aortic pulse wave velocity as a marker of cardiovascular risk in hypertensive patients. *Hypertension* 33, 1111–1117.
- Bland, J.M., Altman, D.G., 1986. Statistical methods for assessing agreement between two methods of clinical measurement. *Lancet* 327, 307–310.
- Cutnell, J.D., Johnson, K., 1998. *Physics*, Fourth ed. Wiley, New York, pp. 308.
- Davies, J.E., Whinnett, Z.I., Francis, D.P., Willson, K., Foale, R.A., Malik, I.S., Hughes, A.D., Parker, K.H., Mayet, J., 2006. Use of simultaneous pressure and velocity measurements to estimate arterial wave speed at a single site in humans. *American Journal of Physiology Heart and Circulatory Physiology* 290, H878–H885.
- Feng, J., Khir, A.W., 2010. Determination of wave speed and wave separation in the arteries using diameter and velocity. *Journal of Biomechanics* 43, 455–462.
- Harada, A., Okada, T., Niki, K., Chang, D., Sugawara, M., 2002. On-line noninvasive one-point measurements of pulse wave velocity. *Heart and Vessels* 17, 61–68.
- Kelly, R.P., Tunin, R., Kass, D.A., 1992. Effect of reduced aortic compliance on cardiac efficiency and contractile function of in situ canine left ventricle. *Circulation Research* 71, 490–502.
- Khir, A.W., O'Brien, A., Gibbs, J.S.R., Parker, K.H., 2001a. Determination of wave speed and wave separation in the arteries. *Journal of Biomechanics* 34, 1145–1155.
- Khir, A.W., Henein, M.Y., Koh, T., Das, S.K., Parker, K.H., Gibson, D.G., 2001b. Arterial waves in humans during peripheral vascular surgery. *Clinical Science* 101, 749–757.
- Khir, A.W., Parker, K.H., 2002. Measurements of wave speed and reflected waves in elastic tubes and bifurcations. *Journal of Biomechanics* 35, 775–783.
- Khir, A.W., Parker, K.H., 2005. Wave intensity in the ascending aorta: effects of arterial occlusion. *Journal of Biomechanics* 38, 647–655.
- Koh, T.W., Pepper, J.R., DeSouza, A.C., Parker, K.H., 1998. Analysis of wave reflections in the arterial system using wave intensity: a novel method for predicting the timing and amplitude of reflected waves. *Heart and Vessels* 13, 103–113.
- McDonald, D.A., 2007. *Blood Flow in Arteries*. Edward Arnold Ltd.
- Meinders, J.M., Kornet, L., Brands, P.J., Hoeks, A.P.G., 2001. Assessment of local pulse wave velocity in arteries using 2D distension waveforms. *Ultrasound Imaging* 23, 199–215.
- Mohiaddin, R.H., Firmin, D.N., Longmore, D.B., 1993. Age-related changes of human aortic flow wave velocity measured noninvasively by magnetic resonance imaging. *Journal of Applied Physiology* 74, 492–497.
- Murgo, J.P., Westerhof, N., Giolma, J.P., Altabelli, S.A., 1980. Aortic input impedance in normal man: relationship to pressure wave forms. *Circulation* 62, 105–116.
- Parker, K.H., Jones, C.J.H., 1990. Forward and backward running waves in the arteries: analysis using the method of characteristics. *Transactions of the ASME, Journal of Biomechanical Engineering* 112, 322–326.
- Rabben, S.I., Stergiopoulos, N., Hellevik, L.R., Smiseth, O.A., Slordahl, S., Urheim, S., Angelsen, B., 2004. An ultrasound-based method for determining pulse wave velocity in superficial arteries. *Journal of Biomechanics* 37, 1615–1622.
- Ramsey, M.W., Sugawara, M., 1997. Arterial wave intensity and ventriculoarterial interaction. *Heart Vessels* 12, 128–134.
- Sun, Y.H., Anderson, T.J., Parker, K.H., Tyberg, J.V., 2000. Wave intensity analysis: a new approach to coronary hemodynamics. *Journal of Applied Physiology* 89, 1636–1644.
- Wang, J.J., Shrive, N.G., Parker, K.H., Tyberg, J.V., 2009. "Wave" as defined by wave intensity analysis. *Medical and Biological Engineering and Computing* 47, 189–195.
- Wang, Z., Jalali, F., Sun, Y.H., Wang, J.J., Parker, K.H., Tyberg, J.V., 2005. Assessment of left ventricular diastolic suction in dogs using wave-intensity analysis. *American Journal of Physiology Heart and Circulation Physiology* 288, H1641–H1651.
- Westerhof, N., Sipkema, P., Van Den Bos, G.C., Elzinga, G., 1972. Forward and backward waves in the arterial system. *Cardiovascular Research* 6, 648–656.